Hall effect in semiconducting epitaxial and amorphous Y-Ba-Cu-O thin films

Pao-Chuan Shan, Agha Jahanzeb, Donald P. Butler,[a] and Zeynep Çelik-Butler
Department of Electrical Engineering, Southern Methodist University, Dallas, Texas 75275

Witold Kula and Roman Sobolewski
Department of Electrical Engineering and Laboratory for Laser Energetics, University of Rochester, Rochester, New York 14627

(Received 30 September 1996; accepted for publication 6 February 1997)

An experimental study of the Hall effect in nonmetallic Y-Ba-Cu-O thin films is reported. Both epitaxial crystalline $YBa_2Cu_3O_{6+x}$ ($x \leqslant 0.5$) and multiphase/amorphous Y-Ba-Cu-O thin films were studied. The structure of the samples was measured by x-ray diffraction and Raman microprobe. The amorphous Y-Ba-Cu-O samples were found to have a grain size of about 100 Å. The conduction properties were studied and analyzed for the two types of samples over a wide temperature range including room temperature. The Hall effect measurements showed positive charge carriers with a concentration ranging from 10^{17} to 10^{20} cm^{-3} at room temperature. The mobility was found to decrease with higher Hall carrier concentration. The empirical relationship for the mobility dependence on impurity concentration agreed with the relationship between mobility and the experimental Hall carrier concentration, suggesting that the same localized states were responsible for both providing the carriers and reducing the mobility through scattering. It was also observed that the mobility values for both amorphous and crystalline samples followed the same empirical curve, a result which showed that the conduction mechanisms in the epitaxial (tetragonal) and amorphous Y-Ba-Cu-O materials are very likely to be similar despite the differences in the composition and structure of the films. The similarity is consistent with other work that concludes that the conduction mechanism occurs along the copper oxide planes. Our work implies that the conduction mechanism operates over a short range, less than the 100 Å grain size of the amorphous, such that the lack of order in the amorphous samples was essentially irrelevant to the charge transport. © *1997 American Institute of Physics.* [S0021-8979(97)04810-X]

I. INTRODUCTION

By appropriately increasing the oxygen content, the phase of $YBa_2Cu_3O_{6+x}$ evolves from that of a Mott-Hubbard insulator ($x \leqslant 0.3$) to a Fermi glass ($0.3 \leqslant x \leqslant 0.5$) and through a semiconductor-metal transition to metallic behavior ($x \geqslant 0.5$).[1] The metallic phase of $YBa_2Cu_3O_{6+x}$ is superconductive with the maximum critical temperature of 92 K for $x \cong 0.9$. During the past decade, most of the studies, as well as proposed applications, have focused almost exclusively on superconductivity in the Y-Ba-Cu-O system.

Recently, the potential application of *semiconducting* Y-Ba-Cu-O thin films as an *uncooled* bolometer was proposed.[2,3] Uncooled infrared detectors, as opposed to, e.g., superconducting Y-Ba-Cu-O bolometers operating using the superconducting-normal state transition,[4–6] do not require refrigeration, and therefore are less costly and easier to implement in commercial applications. Amorphous/mixed phase, semiconducting Y-Ba-Cu-O thin films display a high temperature coefficient of resistance and therefore possess the potential for high responsivity and detectivity values when fabricated into a thermal isolation structure. These films can be deposited by radio frequency (rf) sputtering at ambient temperature, therefore assuring the low cost of detector fabrication and compatibility with complementary metal-oxide-semiconductor (CMOS) technology for focal plane signal processing.

Our investigation of the Hall effect in the multiphase, amorphous semiconducting Y-Ba-Cu-O and tetragonal $YBa_2Cu_3O_{6+x}$ thin films is motivated by the observation that the crystalline films possess a lower temperature coefficient of resistance and by an effort to better understand the underlying conduction mechanism in nonsuperconducting Y-Ba-Cu-O. A clear understanding of the transport behavior of semiconducting Y-Ba-Cu-O is important to the understanding of photoconductivity[1,7] and of the bolometric properties of the material. Furthermore, the transport behavior of the oxygen-deficient semiconducting Fermi-glass state has implications to the transport behavior in metallic oxygen-rich Y-Ba-Cu-O.

The Hall effect has primarily been studied in metallic, superconducting $YBa_2Cu_3O_{6+x}$. These investigations have employed bulk single crystal samples,[8–11] bulk ceramic (polycrystalline) samples,[12–18] and epitaxial thin film samples.[19–26] Investigations at the normal-superconducting transition have revealed an apparent sign reversal in the Hall coefficient, slightly above T_c, near the zero resistance transition.[10,17,18] For the normal state conduction of the metallic $YBa_2Cu_3O_{6+x}$ samples, an ''anomalous,'' yet universal T^2 dependence of the inverse of Hall angle is observed in all the experiments that represents behavior unlike any other known metal. Theoretical investigations[27–30] have been mo-

[a]Author to whom correspondence should be addressed. Electronic mail: dpb@seas.smu.edu

 0021-8979/97/81(10)/6866/8/$10.00

tivated by the anomalous behavior and the impact of the normal state conduction mechanism on the origins of high-T_c superconductivity in the cuprates. Much attention has been devoted to the theoretical framework to explain the T^2 dependence based on the Anderson resonance valence bond (RVB) model of high-T_c superconductivity which assigns the excitations for spin and charge to separate entities, namely chargeless spinons and spinless holons, respectively.[29,31] To a lesser extent, the Hall effect has been investigated in semiconducting Y-Ba-Cu-O samples. In sharp contrast to metallic Y-Ba-Cu-O, the Hall mobility has been observed to *increase* with temperature in semiconducting Y-Ba-Cu-O.[24] This article reports on our investigation of the dependence of the Hall mobility upon the Hall carrier concentration in semiconducting Y-Ba-Cu-O. The Hall effect data are analyzed at room temperature for epitaxial, tetragonal $YBa_2Cu_3O_{6+x}$ and amorphous multiphase Y-Ba-Cu-O thin films. Comparison between the Hall effect implications and the dc resistivity data is also reported.

Following Yu and Heeger,[1] $YBa_2Cu_3O_{6+x}$ is a Mott-Hubbard insulator for $x<0.3$ with a well defined charge transfer gap on the order of 1.5 eV present between the O(2p) band and the Cu(3d) band. The crystal structure is tetragonal with all the O(1) sites vacant. The unit cell consists of three Cu-O planes in the *a-b* plane sandwiched between two planes containing Ba-O and one plane containing Y atoms along the *c* direction. Each layer consists of corner sharing CuO_n polyhedra held together by the Y plane. The polyhedra comprise strong Cu-O bonds whereas the Cu-O bonds bridging the Y plane are weak. As x is increased, O is randomly introduced to the O(1) sites, creating carriers and simultaneously results in disorder, and leading to the formation of localized states in the Cu-O planes. The disorder from the partial oxygenation causes the localization of hole states above the mobility band edge, E_c, and extended hole states for energies below E_c. Thus for the oxygen stoichiometry range of x varying from approximately 0.3 to 0.5, $YBa_2Cu_3O_{6+x}$ displays the electronic characteristic of a Fermi glass. The Fermi energy lies above the mobility band edge by the activation energy $E_A=E_F-E_c\approx 0.18-0.22$ eV. The activation energy decreases with increasing oxygen content until the Fermi energy crosses the mobility band edge E_c for x around 0.5–0.6 in an Anderson metal-insulator transition. Simultaneously, the crystal undergoes a transition to an orthorhombic structure. When the Fermi energy is below the mobility band edge, metallic conductivity is observed with a superconducting transition upon cooling below its critical temperature. The Fermi energy is approximately 0.2 eV below the mobility band edge when the material is fully oxygenated.

The charge transport in the oxygen deficient phase of Y-Ba-Cu-O is thermally activated at sufficiently high temperatures. In this case, the conductivity is dominated by carrier transport in the extended states of the O(2p) band. The carriers are thermally excited from their localized states around the Fermi energy, above the mobility band edge, into the extended states. The resistivity ρ is of the form:

$$\rho=\rho_0 \exp\left(\frac{E_A}{kT}\right), \tag{1}$$

where ρ_0 is the resistivity at the mobility band edge, k is Boltzmann's constant and T is the absolute temperature. At lower temperatures, the carriers lack sufficient thermal energy to be excited into the extended states and conduction occurs by *variable range hopping*. In this case, carriers are randomly excited into the extended states for short periods of time to move from localized state to localized state. Therefore, the temperature dependence of the resistivity is determined by the density of states around the Fermi energy $N(E_F) \propto (E-E_F)^n$ where $n>0$. It can be shown that the resistivity varies with temperature according to the relation[32]

$$\rho=\rho_0 \exp\left(\frac{T_0}{T}\right)^p, \tag{2}$$

where $p=(n+1)/(n+4)$, ρ_0 is a fitting parameter and T_0 is a parameter related to the localization length and the density of states.[32] For a constant three dimensional density of states Eq. (2) reduces to Mott's variable range hopping model[33] with a $\exp(T^{-1/4})$ temperature dependence for the resistivity.

II. EXPERIMENTAL DETAILS

The samples employed in the investigation are listed in Table I. Two types of samples were investigated. The amorphous semiconducting Y-Ba-Cu-O thin films (samples $a-e$) were fabricated at Southern Methodist University[2,3] by rf magnetron sputtering from a 7.5 cm, superconducting, orthorhombic $YBa_2Cu_3O_{6+x}$ sputter target onto 10 cm diameter Si $\langle 100\rangle$ wafers at room temperature. The sputtering was performed using a CVC601 sputtering system at 10 mTorr in an Ar atmosphere. The substrate to target distance was approximately 12 cm. The Si wafers were prepared with different buffer layers as shown in Table I. The SiO_2 layers were thermally wet grown at 1200 °C. The MgO layers were prepared by rf magnetron sputtering from a 20 cm MgO target in an 90% Ar:10% O_2 atmosphere with the substrate at ambient temperature. The use of a SiO_2 layer is relevant to the Si micromachining of thermal isolation structures for the application to uncooled infrared bolometers. The eptitaxial single crystal tetragonal $YBa_2Cu_3O_{6+x}$ thin films (samples f and g) were fabricated at the University of Rochester by rf sputtering onto $LaAlO_3$ substrates at 750 °C to produce a superconducting $YBa_2Cu_3O_{6+x}$ thin film. Later the films were de-oxygenated by annealing in 10 mTorr of Ar at 450 and 680 °C, respectively.[34]

A JEOL 733 Superprobe was used to perform quantitative compositional analysis on our samples employing wavelength dispersive spectrometry (WDS) with thin film correction.[35] The crystal structure of the films was investigated by x-ray diffraction (XRD) and micro-Raman spectroscopy. The Raman effect was used to determine the order in the samples and verify the crystal structure.[36–38] A Renishaw Raman imaging microscope was used with either a HeNe or argon laser in a backscattering configuration with a 1 cm^{-1} spectral and 1 μm spatial resolution.[36] Measurements were performed at room temperature with the laser power kept below 1 mW so as to prevent excessive heating of the thin

TABLE I. Atomic composition and conduction properties of the samples at $T=295$ K ($T=290$ K for sample e) and activation energies E_a found from the relation $R\sim\exp(E_a/kT)$ for selected temperature ranges. All samples are semiconducting.

Sample	Composition	Y:Ba:Cu:O stoichiometry	Structure	I (μA)	ρ (Ω cm)	R_H (cm^3/C)	p_H (cm^{-3})	μ_H (cm^2/V s)	E_a (eV)
a	YBCO(200 nm)-MgO(35 nm)-Si	1.0:0.5:2.0:4.5	amorphous	0.62	19.14	59.58	1.05×10^{17}	3.11	0.248[a]
b	YBCO(200 nm)-Si	1.0:0.3:2.3:4.6	amorphous	6.5	2.81	1.52	4.12×10^{18}	0.54	0.211[b]
c	YBCO(200 nm)-SiO_2(800 nm)-Si	1.0:0.4:2.4:4.6	amorphous	4.85	3.95	3.75	1.67×10^{18}	0.95	0.189[b]
d	YBCO(200 nm)-MgO(35 nm)-SiO_2-Si	1.0:0.5:2.4:4.8	amorphous	4.4	7.42	21.27	2.94×10^{17}	2.87	0.21[b]
e	YBCO(500 nm)-MgO(100 nm)-Si	1.0:0.6:2.3:5.7	amorphous	0.1	34.4	125.72	4.97×10^{16}	3.65	0.214[e]
f	YBCO(200 nm)-$LaAlO_3$	1.0:1.5:2.4:6.5	tetragonal[g]	100.0	0.48	0.07	8.83×10^{19}	0.14	0.034[c]
g	YBCO(200 nm)-$LaAlO_3$	1.0:2.0:2.5:6.3	tetragonal[g]	0.1	50.83	189.12	3.3×10^{16}	3.72	0.148[d]

[a]For 263–318 K.
[b]For 253–318 K.
[c]For 150–320 K.
[d]For 285–320 K.
[e]For 220–310 K.
[f]Measurement techniques: Samples $a-e$: EPMA, samples f, and g: XRD and Raman.
[g]Space group $P4/mmm$.

films. The results of the analysis for samples $a-g$ are shown in Table I. In the case of crystalline samples f and g, the oxygen content given was computed independently from x-ray diffraction data,[39] as discussed in Section III. This latter method provided more realistic results for the oxygen content in these samples and showed that, in general, the oxygen content was overestimated by electron probe microanalysis (EPMA) by about 5%–6%.

Gold leads were attached directly to the film surface by ultrasonic bonding for the electrical measurements. The typical sample geometry was 10×7 mm^2 for samples $a-f$ and 10×4 mm^2 for sample g. A standard four-probe method with a 3 mm spacing was used to measure the resistance of the samples. Samples were mounted in ceramic or Covar packages with colloidal silver paste providing a good thermal contact between the package and the substrate. The package was then attached to the cold finger of a Leybold ROK10-300 cryostat. The temperature control was provided by a LakeShore DRC-91C controller using a calibrated diode sensor. Typical temperature stability was within 8 mK. Electrical measurements were performed over the temperature range of $\sim$250 to 320 K for samples $a-d$, 220–310 K for sample e, 208–320 K for sample g, and 80–320 K for sample f. Since the last was a low-resistivity sample, it could be conveniently biased at low temperatures, whereas it was not possible to bias other samples below 250 K due to their very high resistivities. The Hall effect measurements were performed at room temperature. Magnetic fields up to 1 T were applied to the samples with a Varian 3700 electromagnet while they were current biased in the range of 0.1–100 μA. The geometry for the Hall effect measurements is displayed in Fig. 1. The longitudinal resistivity ρ was measured at points 2 and 3 in the direction of the flow of the current, magnetic field B was applied in the ''z'' direction and the Hall voltage was sensed in the transverse or ''y'' direction. Due to a slight misalignment between probes 5 and 6, there was a non-zero voltage between them when the sample was dc biased in the absence of the B field. To cancel this offset voltage, a potentiometer was attached between points 6 and 7 and adjusted so that $V_{H2\text{-}H1}$, sensed between the wiper of the potentiometer and point 5, was zero before applying the B field. The corrected value of $V_{H2\text{-}H1}$ thus gave us the ''true'' Hall voltage when the B field was applied. The sign of $V_{H2\text{-}H1}$ was observed to be positive implying that the carriers were hole-like. The linearity of the Hall signal was verified by sweeping the magnetic field in z direction up to 1 T (see Fig. 1). The Hall signal was found to be linear in this range for all the samples. To compute the Hall coefficient and, thus, the carrier concentration from the Hall voltage, the latter was averaged for both directions of magnetic field sweep at each applied bias.

III. RESULTS AND DISCUSSION

A. Materials characterization

Figure 2(a) shows a typical XRD pattern from the amorphous Y-Ba-Cu-O films (samples $a-e$) deposited at ambient temperature. Due to the lack of long range crystalline order in these samples, there were no sharp peaks originating from the thin film and the sharp peaks observed were derived from

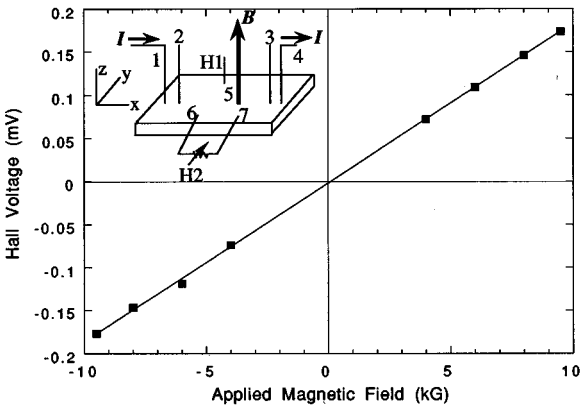

FIG. 1. Magnetic field dependence of the Hall voltage for a typical Y-Ba-Cu-O sample. The case is shown for sample a with $I=0.62$ μA. The inset shows sample geometry for the Hall effect measurement. Hall voltage is determined as $V_H=V_{H2}-V_{H1}$.

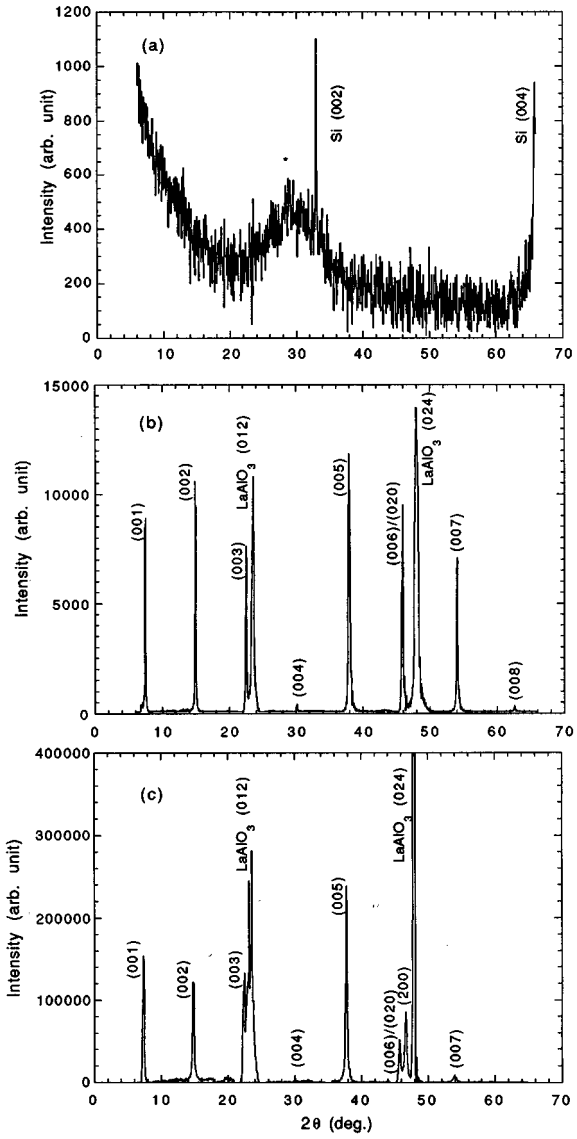

FIG. 2. (a) Typical x-ray diffraction pattern of amorphous Y-Ba-Cu-O thin films. Position marked * could be due to the presence of the Y_2BaCuO_5 phase. (b) XRD pattern for sample f, a single crystal tetragonal $YBa_2Cu_3O_{6+x}$ ($x \sim 0.5$) thin film on $LaAlO_3$ substrate. (c) XRD pattern for sample g, a single crystal tetragonal $YBa_2Cu_3O_{6+x}$ ($x \sim 0.3$) thin film on $LaAlO_3$ substrate.

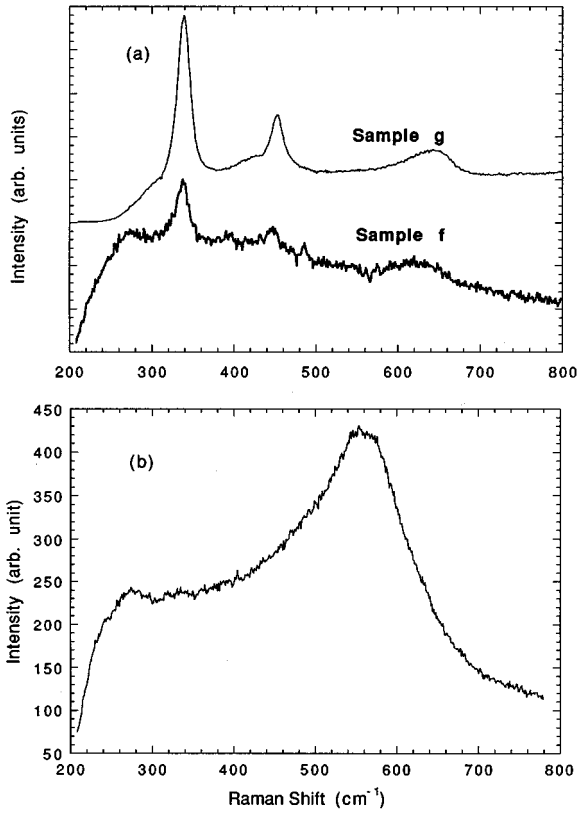

FIG. 3. Raman spectra for Y-Ba-Cu-O samples at room temperature. (a) Spectra for the crystalline samples f and g. (b) A typical Raman spectrum for the amorphous Y-Ba-Cu-O thin films ($a-e$).

the Si substrate. The dominant response from the Y-Ba-Cu-O thin film was a very broad peak at $2\theta \sim 29°$ due to an amorphous film layer with its width [full width at half-maximum (FWHM)] close to 8 °. Scherrer's formula[40] was used to estimate the particle (grain) size in the amorphous Y-Ba-Cu-O films to be approximately 100 Å. The $2\theta \sim 29°$ peak is not a $YBa_2Cu_3O_{6+x}$(123) peak but might be due to the Y_2BaCuO_5 (2115) phase,[41] suggesting the presence of multiple phases in these samples. It has been observed that XRD peaks tend to broaden for materials similar to Y-Ba-Cu-O deposited at lower temperatures due to small grain size.[42] Although increasing the substrate temperature during deposition improves crystallinity (larger grain size) of the material, giving sharper XRD peaks, high temperature processing was avoided in samples $a-e$ since our general intention was to fabricate Y-Ba-Cu-O material suitable for uncooled infrared (IR) detectors and compatible with existing CMOS technology. In fact, crystallinity of Y-Ba-Cu-O is not desired in this application since amorphous films provide higher bolometer figures of merit, i.e., high temperature coefficient of resistance and low $1/f$ noise.[2,3]

Figures 2(b) and 2(c) show the XRD patterns for the semiconducting oxygen-deficient crystalline $YBa_2Cu_3O_{6+x}$ samples f and g, respectively. It can be seen that these films are well oriented the along c axis and possess a tetragonal structure.[43] The average value of the c axis lattice constant was calculated from the angular positions of the various peaks to be approximately 11.85 A° for sample f and 11.89 A° for sample g. Based on these values, we estimated the oxygen content to be about 6.5 ($x=0.5$) for sample f and 6.3 ($x=0.25$) for sample g.[44]

Raman scattering was also used to characterize our samples and to distinguish between the crystalline and the amorphous forms of Y-Ba-Cu-O. Figure 3(a) shows the Raman spectra for samples f and g. The ~ 334 ~ 435, and ~ 500 cm^{-1} bands due to different phonon modes[37,38] can be identified. The 500 cm^{-1} band is due to the Cu-O bond stretch along c axis, whereas the 435 and 334 cm^{-1} bands are due to stretching and bending vibrations in the Cu-O planes. Thomsen *et al.*[38] have shown that the 500 cm^{-1} mode softens and 435 and 334 cm^{-1} modes harden as oxygen is removed from the system. Hence, a reasonable estimate of oxygen content can be made from analyzing these modes in the Raman spec-

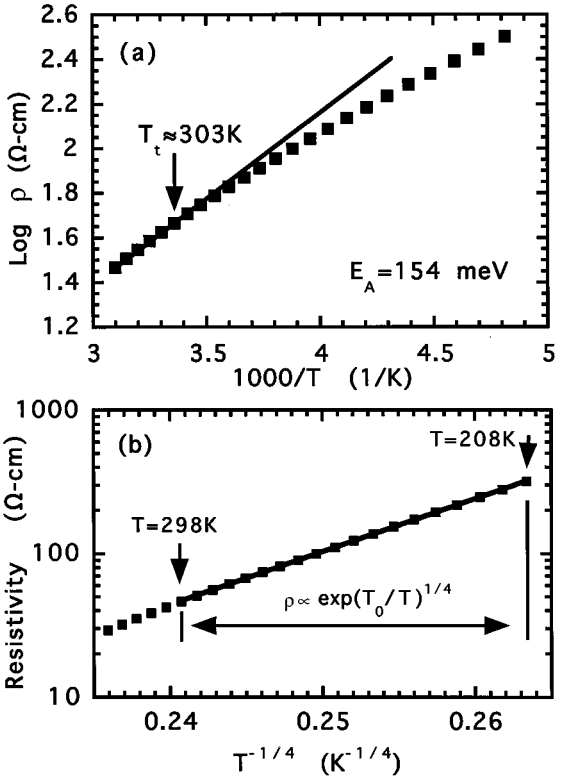

FIG. 4. (a) Arrhenius plot of resistivity for sample f, $YBa_2Cu_3O_{6.3}$. Above approximately 300 K, the conduction shows thermally activated behavior with $E_A \approx 154$ meV. Below 300 K, the local activation energy decreases monotonically. (b) Plotting the natural log of the resistivity vs $T^{-1/4}$ shows a linear relationship below 300 K. This $\exp(T^{-1/4})$ temperature dependence below 300 K is consistent with Mott's variable range hopping model.

tra of our single crystal Y-Ba-Cu-O samples. We observed that the most prominent mode, i.e., 334 cm^{-1}, had shifted to 338 and 339.5 cm^{-1} for f and g, respectively. Using these values and data from Ref. 38, we calculated ''x'' in $YBa_2Cu_3O_{6+x}$ to be 0.45–0.5 and 0.3–0.35 for f and g, respectively. This result is consistent with that obtained from the XRD analysis.

For the amorphous Y-Ba-Cu-O thin films, the Raman spectrum (Fig. 3(b)) consisted of an extremely broad peak around 560 cm^{-1}. This was a very regular feature for all our $a-e$ semiconducting amorphous samples.

B. Hall effect and resistivity data

Table I summarizes the dc resistivity and Hall effect data. All samples $(a-g)$ exhibited semiconducting resistive behavior, i.e., increasing resistance with decreasing temperature with thermally activated transport close to room temperature. Figure 4 shows the resistivity versus temperature behavior of sample f, an epitaxial $YBa_2Cu_3O_{6+x}$ sample. In Fig. 4(a), an Arrhenius plot of the resistivity is shown. Below approximately 300 K, the data deviate from a linear relationship, indicating a departure from thermally activated conductivity. The activation energy was measured from the slope of the Arrhenius plot above 300 K. In Fig. 4(b), the log of the resistivity data is plotted versus $T^{1/4}$. Below approximately 300 K, a linear relationship is observed in the graph indicating that the resistivity of the sample is in agreement with the variable range hopping model. Similar behavior was observed in sample e, although the transition temperature from thermally activated conductivity to hopping conductivity was observed to decrease to 160 K for the sample with the higher oxygen concentration. In the amorphous samples, the resistivity measurements were performed only down to about 250 K. The amorphous samples were observed to remain in the thermally activated region over the entire temperature range despite larger activation energies. It is believed that the lack of long range order in these samples weakened the strength of the localization by considerably broadening the mobility band edge energy E_c. Additional details on the conductivity behavior of the samples can be found in Ref. 45. The presence of a thermally activated conduction mechanism allowed the Hall carrier concentration p_H to be calculated using a single band model, i.e., $p_H = 1/eR_H$, where $R_H = V_H t/BI$ and t is the sample thickness. These values of p_H for semiconducting Y-Ba-Cu-O are understandably lower than what has been observed in metallic Y-Ba-Cu-O at room temperature.[19–26] In addition, a small negative magnetoresistance was observed in all the samples at room temperature which is consistent with a nonhopping type of conductivity.

It is interesting that similar transport features were present in both the amorphous and crystalline Y-Ba-Cu-O samples, despite their difference in structure and composition. A positive Hall coefficient was observed in both types of samples implying that the dominant carriers were holes in both cases. As shown in Table I, the resistivity decreased with an increase in the Hall carrier concentration, a trend that was observed in both amorphous and crystalline samples.

To obtain more information about the carrier scattering mechanism, the Hall mobility ($\mu_H = R_H/\rho$) was calculated. The empirical relationship for carrier mobility[46] was used to fit the experimental data for Hall mobility versus Hall carrier concentration at room temperature for both the amorphous and crystalline Y-Ba-Cu-O samples:

$$\mu_H = \mu_{\min} + \frac{\mu_0}{1 + n_H/N_{\text{ref}}}, \tag{3}$$

where $\mu_{\min} = 0.135$ $cm^2/V\,s$, $\mu_0 = 3.84$ $cm^2/V\,s$, and $N_{\text{ref}} = 5 \times 10^{17}$ cm^{-3} are constants determined by fitting Eq. (3) to the experimental data. In Ref. 46, Arora *et al.* derived Eq. (3) for silicon taking into account lattice and ionized impurity scattering mobilities and electron-electron (hole-hole) scattering mobilities. A temperature dependence was also predicted by considering the temperature dependence of the individual scattering mobilities. Equation (3) has also found modified application to other semiconductors such as GaAs.[47] Figure 5(a) shows the Hall mobility plotted against the Hall carrier concentration using both the actual data and the fit obtained from Eq. (3). Figure 5(b) displays the experimentally measured resistivity versus Hall carrier concentration. Since ρ and μ_H are directly related through $\rho = (q\mu_H p_H)^{-1}$, both plots provide essentially the same information and can be viewed as alternative methods of presenting the data. However, they clearly show that the set of fitting parameters predicts the ρ or, equivalently, the μ_H dependence on p_H with very good accuracy. It is clear from

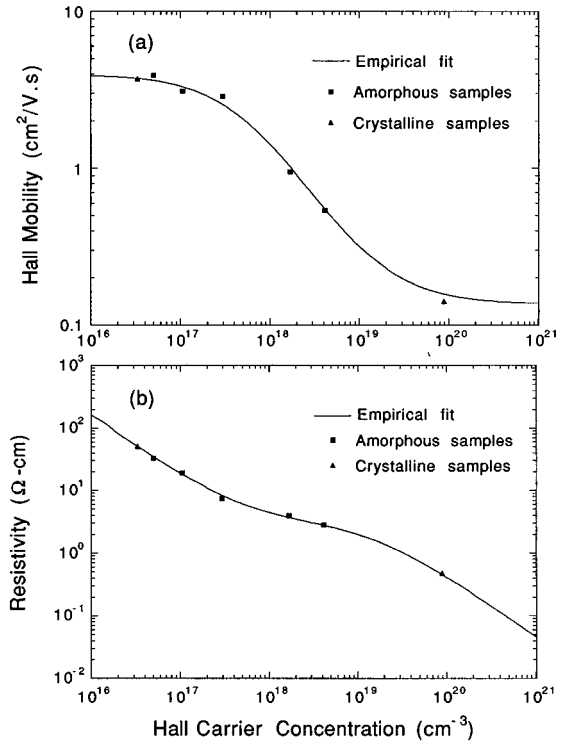

FIG. 5. (a) Hall mobility and (b) dc resistivity vs carrier concentration for the semiconducting thin films at $T=295$ K. The fitting constants for Eq. (3) were determined to be $\mu_{\min}=0.135$ cm^2/V s, $\mu_0=3.84$ cm^2/V s, and $N_{\text{ref}}=5x10^{17}$ cm^{-3}.

Fig. 5 that Eq. (3) provides an appropriate way to relate μ_H to the p_H for both the amorphous and crystalline samples.

The empirical-fit relation suggests that the impurities in a semiconductor act as scattering centers. If the impurity concentration is sufficiently low, the impurities do not limit the mobility of the carriers and the mobility is determined by lattice (phonon) scattering. As the impurity concentration is increased, the carriers are increasingly scattered by the impurities. The result is a reduction in the mobility of the carriers as the mobility becomes dominated by impurity scattering.

In our case, the striking result is that the mobility of the amorphous Y-Ba-Cu-O and tetragonal Y-Ba-Cu-O samples follow the same empirical-fit relation. In fact, the two tetragonal Y-Ba-Cu-O samples have the highest and lowest carrier concentrations of the samples investigated and represent the upper and lower bounds for our amorphous films. The similarity in the conductivity behavior occurs despite the fact the two groups of samples possess different stoichiometries and different long range crystalline order. This result implies that the mechanism of conductivity in the amorphous samples is similar to that in the tetragonal samples. The following explanation is proposed. The carriers in the amorphous samples must be predominantly moving along CuO_2 planes, as in the case of the tetragonal samples. The similarity of the activation energies suggests that oxygen serves as the acceptor impurity, donating hole carriers to move along the CuO_2 planes, in both cases, and the lack of long range order in the amorphous samples does not appear to be affecting the conduction mechanism. Therefore the conduction mechanism must be very short range, likely much less than the 100 Å particle size contained in the films. The low value of the Hall mobility supports our argument for short range conduction.

As in the case of Si, the Hall mobility of the Y-Ba-Cu-O samples decreases with increasing Hall carrier concentration [see Fig. 5(a)]. This suggests that the number of scattering centers also increases with the Hall carrier concentration. Therefore, oxygen not only contributes hole carriers to the system[1,48] it, at the same time, serves as the dominant source of scattering centers. This explanation seems to hold true for the crystalline samples f and g, which lie at the two extremes on the mobility curve. For the amorphous samples $a-e$, represented by the intermediate values on the mobility curve, the situation is less straightforward. First, the compound species present in these samples are difficult to identify. Second, the presence of multiple phases complicates the analysis and, finally, the samples are likely to be polycrystalline on a very fine scale (100 Å). However, since the sputtering target had the robust stoichiometry of 123, and we saw some evidence of the 2115 phase from XRD, we can assume that our amorphous samples contain primarily 123 (with oxygen stoichiometry sufficiently low to give semiconducting behavior) and 2115 phases. The common feature of both the amorphous and crystalline samples is the presence of CuO_2 planes in their structure. It is well known that planes play a dominant role in conduction mechanism[1] in 123 Y-Ba-Cu-O. Even when the long range crystalline order is absent, these planes are present on the microscale and allow conduction to take place in a manner similar to a well-ordered material. Hole carriers are formed in these layers when electrons are transferred to the Cu-O charge reservoir chains because of Cu^{3+} average charge at Cu chain sites. As the number of carriers increases, the mobility decreases and simultaneously the resistivity of the sample decreases. The concentration of carriers should therefore give an approximate picture of the phase of the system, i.e., whether it is metallic or semiconducting. Increasing the oxygen content causes the addition of more holes in the system and thereby changes the phase from semiconducting to metallic.

As the oxygen concentration is increased to form metallic Y-Ba-Cu-O, the Fermi energy crosses the mobility band edge and the variation in the Hall mobility with oxygen or carrier concentration is no longer predicted by the empirical mobility formula. Raven and Wan[26] have shown that the Hall mobility of metallic $YBa_2Cu_3O_{6+x}$ can increase, decrease, or remain essentially constant with oxygen concentration. Raven and Wan proposed that the variation of the Hall mobility with oxygen concentration was dependent upon the method of sample fabrication and the resultant subtle variations in the microstructure of metallic Y-Ba-Cu-O, perhaps causing subtle changes in the dominant transport mechanism. In contrast, the Hall mobility of semiconducting Y-BaCu-O, existing in a Fermi glass state, does not depend upon the gross microstructure. Therefore, the same empirical formula predicts the dependence of the Hall mobility upon carrier concentration in both single crystal and amorphous thin film samples. In general, the reported Hall mobility of metallic

Y-Ba-Cu-O is higher than the low value observed at high carrier concentrations in semiconducting Y-Ba-Cu-O, suggesting that the Hall mobility must increase as the Y-Ba-Cu-O undergoes a phase transition from a semiconducting to a metallic state. This result is not surprising since the microstructure undergoes a transition from tetragonal to orthorhombic. Simultaneously, the Fermi energy crosses the mobility edge[1] at the phase transition causing the carriers to sample a different portion of the conduction band.

IV. CONCLUSION

We investigated the carrier and transport properties of semiconducting crystalline and amorphous Y-Ba-Cu-O thin films. Material analysis showed that samples appearing amorphous on a broad scale were actually multiphase and polycrystalline on a very fine scale, while the epitaxial crystalline samples were tetragonal with oxygen contents of 6.5 and 6.3, respectively. At room temperature, all our samples exhibited thermally activated conduction behavior. At reduced temperatures, the crystalline samples underwent a transition to variable range hopping at temperatures of approximately 300 and 160 K for samples *f* and *g*, respectively. No transition to hopping conduction was observed for the amorphous samples, although these samples were only cooled to 250 K. We interpret the difference in the behavior of the amorphous sample over this temperature range to be a consequence of the lack of long range order, weakening the strength of the localization and being associated with the considerable broadening of the mobility band edge energy E_c. The Hall voltage increased linearly with increasing magnetic field. The dependence of the Hall mobility and resistivity of the samples on Hall carrier concentration was very accurately in accord with the mobility empirical-fit formula. This fit indicates that oxygen in Y-Ba-Cu-O is not simply the acceptor impurity providing carriers for conduction, but also the *dominant* source of impurity scattering. The Hall mobility and dc resistivity for both amorphous and crystalline samples followed the same relationship in terms of Hall mobility dependence on Hall carrier concentration, demonstrating that the conduction mechanism in semiconducting Y-Ba-Cu-O is dominated by CuO_2 planes and is very short ranged (less than 100 Å), since the lack of long range order in the amorphous samples did not lead to a different mobility behavior when compared to the epitaxial crystalline thin films.

ACKNOWLEDGMENTS

This work was supported in part by the National Science Foundation under Grant Nos. ECS-9460961 (SMU) and ECS-9421969 (SMU), by the Army Research Office under Grant No. 33848PH (SMU) and by the AFOSR under Grant No. F49620-94-1-0094 (University of Rochester). The authors would like to thank Dwight Deuring for help with XRD and microprobe measurements. They are also grateful to Andrew Whitley and Ken Williams of Renishaw plc (U.K.) and David Caplin and Y. B. Li at Imperial College (U.K.) for help with Raman spectroscopic analysis.

[1] G. Yu and A. J. Heeger, Int. J. Mod. Phys. B **7**, 3751 (1993).
[2] P. C. Shan, Z. Çelik-Butler, D. P. Butler, and A. Jahanzeb, J. Appl. Phys. **78**, 7334 (1995).
[3] P. C. Shan, Z. Çelik-Butler, D. P. Butler, A. Jahanzeb, C. M. Travers, W. Kula, and R. Sobolewski, J. Appl. Phys. **80**, 7118 (1996).
[4] S. Verghese, P. L. Richards, K. Char, and S. A. Sachtjen, IEEE Trans. Magn. **27**, 3077 (1992).
[5] B. R. Johnson, T. Ohnstein, C. J. Han, R. Higashi, P. W. Kruse, R. A. Wood, H. Marsh, and S. B. Dunham, IEEE Trans. Appl. Supercond. **3**, 2856 (1993).
[6] J. C. Brasunas and B. Lakew, Appl. Phys. Lett. **64**, 777 (1994).
[7] C. Stockinger, W. Markowitsch, W. Gob, W. Lang, W. Kula, and R. Sobolewski, Applied Superconductivity 1995, Vol. 2, Proceedings of EUCAS 1995, The Second European Conference on Applied Superconductivity, edited by D. Dew-Hughes (IOP, Bristol, UK, 1995), p. 975.
[8] N. W. Preyer, R. J. Birgeneau, C. Y. Chen, D. R. Gabbe, H. P. Jenssen, M. A. Kastner, P. J. Picone, and T. Thio, Phys. Rev. B **39**, 11 563 (1988).
[9] M. D. Lan, J. Z. Liu, Y. X. Jia, L. Zhang, and R. N. Shelton, Phys. Rev. B **49**, 580 (1994).
[10] J. P. Rice, N. Rigakis, D. M. Ginsberg, and J. M. Mochel, Phys. Rev. B **46**, 11 050 (1992).
[11] L. Forro and A. Hamzic, Solid State Commun. **71**, 1099 (1989).
[12] G. Kalhas, I. Panagiotopoulos, D. Niarchos, and A. Kostikas, Phys. Rev. B **48**, 15 992 (1993).
[13] M. F. Hundley, A. Zettl, A. Stacy, and M. L. Cohen, Phys. Rev. B **35**, 8800 (1987) for early work on related material $La_{1.85}Sr_{0.15}CuO_4$.
[14] G. Priftis, A. M. Ghorayeb, O. Gorochov, R. Suryanarayanan, H. Pankowska, and M. Rateau, Physica C **162–164**, 1201 (1989).
[15] G. Ilonca, M. Mehbod, A. Lanckbeen, and R. Deltour, Phys. Rev. B **47**, 15 285 (1993).
[16] M. Affronte, J. Y. Genoud, T. Graf, M. Decroux, and O. Fischer, Phys. Rev. B **45**, 8189 (1992).
[17] G. C. Vezzoli, T. Burke, B. M. Moon, B. Lalevic, A. Safari, H. G. K. Sundar, R. Bonometti, C. Alexander, C. Rau, and K. Waters, J. Magn. Magn. Mater. **79**, 146 (1989).
[18] G. C. Vezzoli, M. F. Chen, F. Craver, A. Safari, B. M. Moon, B. Lalevic, T. Burke, and M. Shoga, J. Magn. Magn. Mater. **88**, 351 (1990).
[19] P. Xiong, G. Xiao, and X. D. Wu, Phys. Rev. B **47**, 5516 (1993).
[20] B. Wuyts, E. Osquiguil, M. Maenhoudt, S. Libbrect, Z. X. Gao, and Y. Bruynseraede, Phys. Rev. B **47**, 5512 (1993).
[21] A. Carrington, D. J. C. Walker, A. P. Mackenzie, and J. R. Cooper, Phys. Rev. B **48**, 13 051 (1993).
[22] R. Hopfengartner, M. Leghissa, G. Kreiselmeyer, B. Holzapfel, P. Schmitt, and G. Saemann-Ischenko, Phys. Rev. B **47**, 5992 (1993).
[23] E. C. Jones, D. K. Christen, J. R. Thompson, R. Feenstra, S. Zhu, D. H. Lowndes, J. M. Phillips, M. P. Siegal, and J. D. Budai, Phys. Rev. B **47**, 8986 (1993).
[24] A. Jahanzeb, Z. Çelik-Butler, P. C. Shan, and D. P. Butler, J. Appl. Phys. **78**, 6658 (1995).
[25] W. Lang, G. Heine, P. Schwab, X. Z. Wang, and D. Bauerle, Phys. Rev. B **49**, 4209 (1994).
[26] M. S. Raven and Y. M. Wan, Phys. Rev. B **51**, 561 (1995).
[27] A. S. Alexandrov, A. M. Bratkovsky, and N. F. Mott, Semicond. Sci. Technol. **6**, 755 (1993).
[28] D. Y. Xing and C. S. Ting, Phys. Rev. B **38**, 5134 (1988).
[29] A. J. Schofield and J. M. Wheatley, Phys. Rev. B **47**, 11 607 (1993).
[30] P. W. Anderson, Science **256**, 1526 (1992).
[31] P. W. Anderson and D. Khveshchenko, Phys. Rev. B **52**, 16 415 (1995).
[32] B. I.Shklovskii and E. L. Efros, *Electronic Properties of Doped Semiconductors* (Springer, Berlin, 1984).
[33] N. F. Mott and E. A. Davis, *Electronic Processes in Non-crystalline Materials*, (Clarendon, Oxford, 1979).
[34] R. Sobolewski, W. Xiong, W. Kula, and J. R. Gavaler, Appl. Phys. Lett. **64**, 643 (1994).
[35] R. A. Waldo, in *Microbeam Analysis*, edited by D. E. Newbury (San Francisco Press, San Francisco, 1988). p. 310.
[36] Y. B. Li, C. Shelley, L. F. Cohen, A. D. Caplin, R. A. Stradling, W. Kula, R. Sobolewski, and J. L. MacManus-Driscoll, Physica C **80**, 2929 (1996).
[37] F. E. Bates, Phys. Rev. B **39**, 322 (1989).
[38] C. Thomsen, R. Liu, M. Bauer, A. Wittlin, L. Genzel, M. Cardona, E. Schönherr, W. Bauhofer, and W. Konig, Solid State Commun. **65**, 55 (1988).
[39] J. D. Jorgensen, B. W. Veal, A. P. Paulikas, L. J. Nowicki, G. W. Crabtree, H. Claus, and W. K. Kwok, Phys. Rev. B **41**, 1863 (1990).

[40] B. D. Cullity, *Elements of X-ray Diffraction*, 2nd ed. (Addison-Wesey, Reading, MA, 1978).
[41] Q. Y. Ma, M. T. Schmidt, T. J. Licate, D. V. Rossi, E. S. Yang, C. Chan, and C. E. Farrell, in *Superconductivity and Applications*, edited by H. S. Kwok, Y. H. Kao, and D. T. Shaw (Plenum, New York, 1989), p. 175.
[42] G. Jakob, V. V. Moshchalkov, and Y. Bruynseraede, Appl. Phys. Lett. **66**, 2564 (1995).
[43] Q. G. He, F. Lin, D. Chang, M. Eschwei, and W. C. Wang, Physica C **184**, 295 (1991).
[44] E. Osquiguil, M. Maenhoudt, B. Wuyts, and Y. Bryuynseraede, Appl. Phys. Lett. **60**, 1627 (1992).
[45] Z. Çelik-Butler, D. P. Butler, A. Jahanzeb, C. M. Travers, W. Kula, and R. Sobolewski, Solid-State Electron. (to be published).
[46] N. D. Arora, J. R. Hauser and D. J. Roulston, IEEE Trans. Electron Devices **ED-29**, 292 (1982).
[47] R. F. Pierret, *Advanced Semiconductor Fundamentals* (Addison-Wesley, Reading, MA, 1987).
[48] J. D. Jorgensen, Phys. Today **44**, 34 (1991).